In presenting the dissertation as a partial fulfillment of the requirements for an advanced degree from the Georgia Institute of Technology, I agree that the Library of the Institute shall make it available for inspection and circulation in accordance with its regulations governing materials of this type. I agree that permission to copy from, or to publish from, this dissertation may be granted by the professor under whose direction it was written, or, in his absence, by the Dean of the Graduate Division when such copying or publication is solely for scholarly purposes and does not involve potential financial gain. It is understood that any copying from, or publication of, this dissertation which involves potential financial gain will not be allowed without written permission.

7/25/68

AN INVESTIGATION OF THE SMALL UNDULAR SURGE IN A HORIZONTAL CHANNEL OF CIRCULAR CROSS SECTION

A THESIS

Presented to

The Faculty of the Graduate Division

by

James Franklin Adams

In Partial Fulfillment

of the Requirements for the Degree

Master of Science in Civil Engineering

Georgia Institute of Technology

August, 1969

AN INVESTIGATION OF THE SMALL

UNDULAR SURGE IN A HORIZONTAL

CHANNEL OF CIRCULAR CROSS SECTION

Approved:

Chairman

Date approved by Chairman: September 3, 1969

PREFACE

The author wishes to express his gratitude to Dr. M. R. Carstens, the thesis advisor, both for the concept of study and his guidance during the execution of the program; to Mr. H. J. Bates for his help in the construction of the equipment; and to Dr. G. M. Slaughter and Dr. C. S. Martin for their help in preparing the manuscript.

The author dedicates this thesis to his wife, Brenda C. Adams, whose love, understanding, and encouragement made this effort possible.

TABLE OF CONTENTS

LIST OF TABLES

LIST OF ILLUSTRATIONS

SUMMARY

In an open channel, a rapidly changed condition which results in either an increase in discharge upstream or a decrease in discharge downstream is transmitted throughout the system by a steep-fronted gravity wave called a positive surge, or bore. The depth transition exhibited by one form of the positive surge is characterized by a smooth undulating surface. Various engineers have studied the undular surge in channels of uniform depth (rectangular channels) and have shown that the control volume analysis, utilizing the equations of continuity and linear momentum, predicts accurately the wave celerity when the end sections are taken in the uniform depth regions ahead and behind the surge. However, only a limited number of studies have been performed in which positive surges were studied in nonrectangular channels.

The writer investigated experimentally the characteristics of small undular surges in a channel of circular cross-section and horizontal slope. Small undular surges were generated into still water by a plane piston of constant velocity. The geometry of the cross-section was changed by varying the initial still-water depth. The velocity of the plane piston was maintained approximately constant throughout the experiments.

As a result of the experiments with a positive surge in a circular-segment open channel in which cross-channel transfers of linear momentum exist through the surge, the writer found that the control volume analysis was valid in nonrectangular channels and that the hydraulic mean depth,

y_m = A/T, was a valid depth to be used in the computation of wave celerity and Froude numbers.

CHAPTER I

INTRODUCTION

In liquids with a free surface, the gravity wave is the physical mechanism by which changed conditions at any point are transmitted throughout the entire system. Since the engineer is often concerned with the response characteristics of an open-channel or stream to change, he is required to understand gravity-wave characteristics by which changing conditions are relayed throughout a given system. Since the wave characteristics are influenced by channel geometry and boundary shear, and since an infinite number of waves are emitted theoretically from a continuously changing boundary condition, the prediction of the response of a system is very difficult. At the current time (1969), many research workers are investigating numerical techniques by means of which the engineer can predict the response of an open-channel-flow system such as the prediction of stages as a flood moves downstream in a river.

One type of gravity wave which is amenable to analysis is the positive surge in which the water depth following the wave is greater than the water depth preceding the wave. The rear portions of the positive surge tend to overrun the front portions resulting in a total wave which is relatively short. If the effect of the boundary-shear force is negligible, the celerity and geometric form of the positive surge will remain constant as the surge moves along a uniform channel. These features of the positive surge permit an analytical solution

for the celerity utilizing the equations of continuity and linear momentum with a control volume for which the end sections are in the uniform depth regions in front and behind the surge. Of course, this gross streamtube analysis yields no information about the non-uniform flow conditions within the control volume. In other words, experiments are required for determining the water-surface profile of a positive surge.

The positive surge in a rectangular channel has been extensively studied experimentally because of the occurrence in stilling basins and in the tailraces of hydroelectric generating plants when the turbine discharge is increased rapidly. The principal characteristics of the positive surge are summarized in all open-channel-flow references such as in Engineering Hydraulics (1). Binnie and Orkney (2) classified positive surges into three types as follows:

(a) smooth undular, $y_2/y_1 < 1.35$;

(b) broken undular, $1.35 < y_2/y_1 < 1.75$;

(c) breaking, $1.75 < y_2/y_1$,

in which y_1 and y_2 are the flow depths before and after the surge respectively. The smooth undular surge exhibits several undulations about the following depth y_2. The broken undular surge is similar except that the leading undulation is broken near the crest. The breaking surge is characterized by breaking which extends completely down the face of the leading wave and by the absence of following undulations. Sandover and Zienkiewicz (3) studied the free surface profiles of positive surges in rectangular channels. They found that the height

above the channel bottom of the leading crest of a smooth undular surge is approximately equal to the crest height above the channel bottom of a solitary wave moving with the same celerity.

A limited number of studies have been performed in which surges were studied in nonrectangular channels. Lane and Kindsvater (4) experimented with a stationary positive surge in a circular pipe. The surges in these experiments were all of the breaking type in which the pipe was completely filled following the surge. No surface profiles were determined. The principal conclusion was that control-volume analysis involving the equations of continuity and linear momentum (boundary-shear force neglected) was closely verified.

Sandover and Taylor (5) studied positive surges (undular) in trapezoidal channels. Their three channels differed in side slopes, that is, 30, 45, and 60 degrees. A positive surge was induced by rapidly opening a supply-line valve leading to the trapezoidal channel containing still water. Surge profiles were measured from strip-chart records of capacitance depth gages. One result of this work was to demonstrate the variation of water-surface profiles at various distances from the center line. They observed that different classifications of surge profiles could occur in the same surge.

A similar observation was made by Wilroy (6) who studied a stationary positive surge in a trapezoidal channel with vertical sidewalls. The bottom slope perpendicular to the direction of flow was 1 (vertical) on 3 (horizontal). In one run the surge profile was smooth undular near to the deep side, broken undular in mid-channel, and breaking near the shallow side. In spite of the varying depths in

the transverse direction, surge celerity was constant since Wilroy obtained a stationary surge which was perpendicular to the direction of flow. Wilroy pointed out that the existence of a positive surge in a channel of varying depths in the transverse directions requires a cross-channel transfer of linear momentum toward the shallow side.

Rodrigues-Diaz (7) continued the studies on the stationary positive surge utilizing the same equipment that had been used by Wilroy. He found that the surge front was curved in plan except when a breaking surge existed entirely across the channel. The breaking portion of the surge front was always perpendicular to the direction of flow even when the surge was undular on the deep side and breaking on the shallow side. If the depths were too small on the shallow side, Rodrigues-Diaz found that the character of surge changed with large vertical eddies being formed on the shallow side. He interpreted this new phenomenon as being the result of the necessity of large cross-channel transfers of linear momentum toward the shallow side. In spite of the variety of features exhibited in the trapezoidal channel, Rodrigues-Diaz found that surge celerity could be calculated from the linear momentum (neglecting the boundary-shear force) and continuity equations applied to the entire stream section.

With channels of nonrectangular cross section, the usual practice is to use an effective depth for the entire cross section. The value of the effective depth, y_m, (hereafter referred to as the mean depth) is obtained by dividing the cross sectional area, A, by the top width, T. Only in a rectangular channel is the mean depth, y_m, equal to the actual depth, y, across the channel. In a rectangular

channel the Froude number, $\mathbb{F}$, is interpreted as the ratio of the velocity, V, in the channel to the celerity of an elementary gravity wave, c, in which $c = \sqrt{gy}$. In rectangular channels values of $\mathbb{F} > 1$ are associated with supercritical flow and of $\mathbb{F} < 1$ are associated with subcritical flow. Presumably the same connotation applies to non-rectangular channels, that is, when $V/\sqrt{gy_m} > 1$ the flow is supercritical and when $V/\sqrt{gy_m} < 1$ the flow is subcritical.

A uniform channel in which the wetted perimeter is an arc of a circle is peculiar when interpreted in terms of the effective depth, y_m. First, the value of y_m approaches infinity as the water surface approaches the top of the circular conduit. If the Froude-number interpretation given above is valid, the implication is that super-critical open-channel flow is impossible in a circular conduit when the conduit is flowing nearly full. Second, the value of y_m exceeds the maximum depth in the channel whenever the maximum depth exceeds 0.77 times the conduit diameter, D.

Because of the odd interpretations which result from the use of the mean depth, y_m, the writer decided to investigate open-channel flow in a circular-segment open channel. The analytical investigation is limited to control-volume analysis of a positive surge by means of the continuity and linear-momentum equations. The experimental study was limited to the smooth-undular positive surge in a circular pipe. Surges were generated by a plane piston which was moved at a constant velocity, V_p. The surge moved into still water. By using a circular conduit changes in channel geometry could be made by varying the initial still-water depth.

CHAPTER II

THEORY

A sketch of a vertical-cross-section of a smooth-undular positive surge moving into still water is shown in Figure 1. The fluid velocity, V_1, ahead of the surge is zero since the water in the conduit is initially still. The surge moves with the wave velocity, V_w, in the direction shown by the arrow. The channel cross section, designated as section 2, is assumed to be sufficiently far behind the surge so that the velocity, V_2, can be assumed to be nearly uniform. Admittedly, the length from the toe of the surge to section 2 may be quite long inasmuch as the initially still water which is overrun by the surge must be entrained and mixed with the overlying water in order to attain the uniform-flow conditions assumed at section 2. The force, F_f, is the boundary-shear force exerted by the conduit walls on the fluid contained between sections 1 and 2. Because the wave is moving from right to left in Figure 1, the motion is unsteady.

Two continuity equations can be written for the surge condition illustrated in Figure 1. First

$$V_2 A_2 = V_w (A_2 - A_1) \tag{1}$$

and second

$$V_2 A_2 = V_p A_2 \tag{2}$$

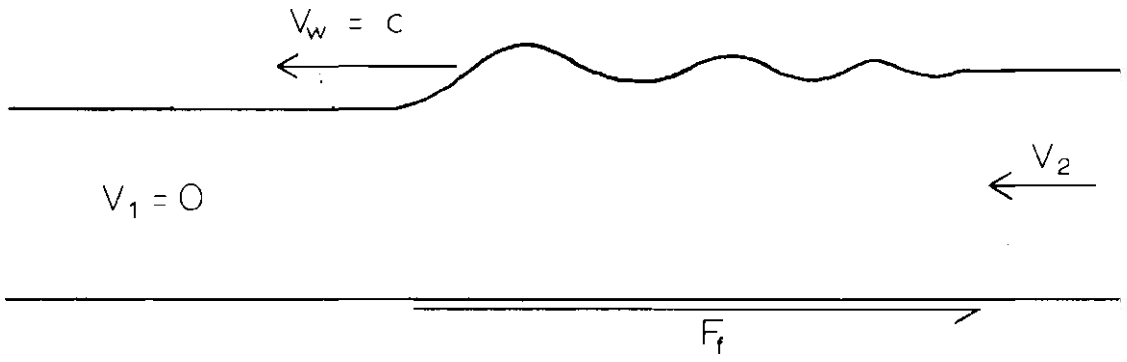

Figure 1. Positive Surge Moving into Still Water.

Equation 2 is predicated on the assumption that the water-contact area, A_p, on the face of the piston is equal to the cross sectional area, A_2. Inasmuch as the boundary-shear force opposes the fluid motion between section 2 and the face of the piston, A_p will be somewhat greater than A_2 and the water surface will slope downward from the piston to section 2. Hence Equation 2 is approximately true only if the distance between section 2 and the piston is limited. Solving for the wave velocity from Equations 1 and 2

$$V_w = V_p\left(\frac{A_2}{A_2 - A_1}\right) \tag{3}$$

which shows that the wave velocity, V_w, is always greater than the piston velocity, V_p. In this case the surge moves into still water, with the result that the wave velocity, V_w, is equal to the wave celerity, c. Wave celerity is the speed of the wave relative to the approaching flow.

Assuming that the surge moves at a constant velocity, V_w, or celerity, c, and with a constant form (profile), the unsteady motion can be analyzed as a steady motion by attaching the coordinate system to the surge front as shown in Figure 2. Relative to the wave, the velocity at section 1 is c from left to right. Relative to the wave, the velocity at section 2 is $c - V_2$ from left to right as shown in Figure 2. In this frame of reference the discharge is

$$Q_r = cA_1 \tag{4a}$$

and

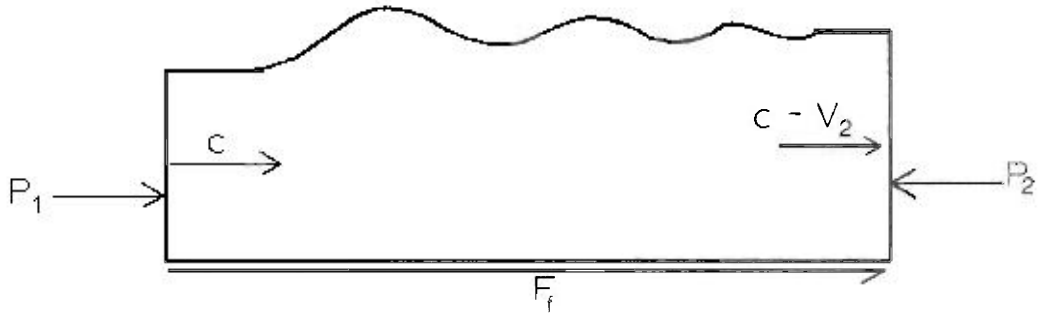

Figure 2. Control Volume (Relative to Surge Front).

$$Q_r = (c - V_2)\, A_2 \tag{4b}$$

In this frame of reference, the linear momentum equation in the direction of flow is

$$P_1 - P_2 + F_f = \rho Q_r (c - V_2) - \rho Q_r (c) \tag{5}$$

in which ρ is the liquid density, in which P_1 and P_2 are the pressure forces at sections 1 and 2, respectively, and in which F_f is the boundary-drag force. Since sections 1 and 2 are assumed to be far enough away from the wave front to be in nearly uniform flow zones, the pressure distribution is hydrostatic with the result that the pressure force P can be replaced with the well-known relation, $\gamma \bar{y} A$, in which γ is the specific weight of the water, $\bar{y}$ is the vertical distance from the water surface to the centroid of the cross section, and A is the area of the cross section. Substituting for the pressure forces in, neglecting the boundary-shear force in, and eliminating Q_r and V_2, (by means of Equations 4a and 4b) from Equation 5

$$\gamma \bar{y}_1 A_1 - \gamma \bar{y}_2 A_2 = \frac{\rho c^2 A_1^2}{A_2} - \rho c^2 A_1 \tag{6}$$

Solving for wave celerity from Equation 6

$$c = \sqrt{g \bar{y}_1}\, \frac{\left(\frac{A_2 \bar{y}_2}{A_1 \bar{y}_1} - 1 \right)^{\frac{1}{2}}}{\left(1 - \frac{A_1}{A_2} \right)^{\frac{1}{2}}} \tag{7}$$

For the circular-segment cross section as shown in Figure 3, the quantities A and $\bar{y}$ are as follows

$$A = \frac{D^2}{4} (\alpha - \sin \alpha \cos \alpha) \tag{8}$$

and

$$\bar{y} = \frac{D}{2} \left\{ \frac{2 \sin^3 \alpha}{3(\alpha - \sin \alpha \cos \alpha)} - \cos \alpha \right\} \tag{9}$$

in which α and the maximum depth y are related as follows

$$\cos \alpha = \frac{(D/2) - y}{D/2} = 1 - 2 \frac{y}{D} \tag{10}$$

Rather than solving for the celerity, Equation 7, an alternative analysis is to derive an expression for the sum of the pressure force and linear-momentum flux at a section. This sum is commonly called pressure-plus-momentum, P + M. Substituting for the pressure forces in, neglecting the boundary-shear force in, and eliminating c and V_2 from Equation 5

$$\gamma \bar{y}_1 A_1 - \gamma \bar{y}_2 A_2 = \frac{\rho Q_r^2}{A_2} - \frac{\rho Q_r^2}{A_1} \tag{11}$$

Transposing

$$\gamma \bar{y}_1 A_1 + \frac{\rho Q_r^2}{A_1} = \gamma \bar{y}_2 A_2 + \frac{\rho Q_r^2}{A_2} \tag{12}$$

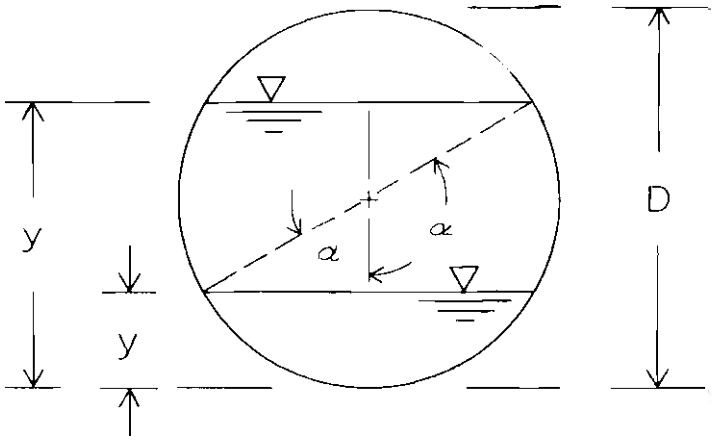

Figure 3. Circular-Segment Cross Section.

Thus

$$(P + M)_1 = (P + M)_2 \tag{13}$$

before and after a positive surge provided that the frame of reference moves with the surge. From Equation 12 for any uniform channel

$$P + M = \gamma \bar{y} A + \frac{\rho Q_r^2}{A} \tag{14}$$

and for a uniform channel with a circular-segment cross section

$$P + M = \frac{\gamma D^3}{8}(\alpha - \sin\alpha\cos\alpha)\left\{\frac{2\sin^3\alpha}{3(\alpha - \sin\alpha\cos\alpha)} - \cos\alpha\right\} + \frac{\frac{1}{2}\rho Q_r^2}{D^2(\alpha - \sin\alpha\cos\alpha)} \tag{15}$$

In dimensionless form, Equation 15 can be written as

$$\frac{P - M}{\gamma D^3} = \frac{(\alpha - \sin\alpha\cos\alpha)}{8}\left\{\frac{2\sin^3\alpha}{3(\alpha - \sin\alpha\cos\alpha)} - \cos\alpha\right\} + \frac{4 Q'^2}{(\alpha - \sin\alpha\cos\alpha)} \tag{16}$$

in which

$$Q' = \frac{Q_r}{\sqrt{gD^5}} \tag{17}$$

Equation 16 is plotted in Figure 4 for seven different values of Q'. In Figure 4 the ordinates are y/D rather than α as in Equation 16. Equation 10 is the geometric function relating α and y/D. The dashed line in Figure 4 passes through the minimum value of P + M depicting the critical-depth ratio, y_c/D. In accordance with Equation 13, a positive surge is depicted in Figure 4 by the intersection of a vertical straight line with the curve of constant Q'. The intersection at the smaller value of y/D is the depth ratio before the surge and the larger value is the depth ratio behind the surge. If the depth ratio before the surge, y_1/D, lies to the right and below the lower cross-hatched curve, the flow behind the surge will be enclosed flow. The region of interest in this study lies between the two cross-hatched curves, that is, where $y_2/D < 1$.

The peculiarity that supercritical flow is theoretically impossible as the depth, y, approaches the top of the circular conduit is shown in Figure 5. As y_c/D approaches unity the value of Q' approaches infinity. Since both g and D in the denominator of Q' are finite, the discharge Q_r would tend to be infinite. Hence supercritical flow is theoretically impossible as the depth approaches the top of the conduit regardless of the slope of the conduit.

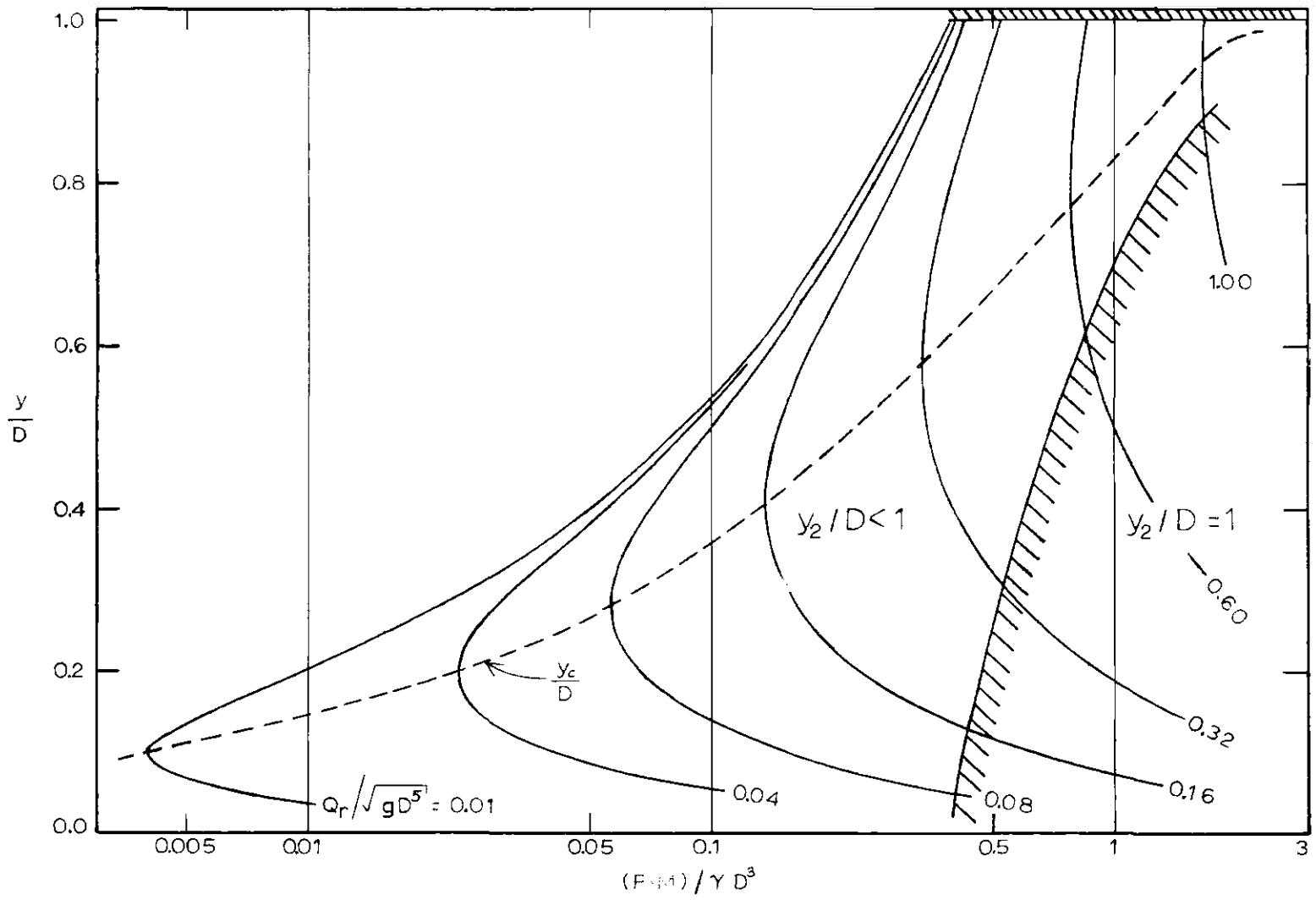

Figure 4. Pressure-plus-Momentum in a Circular Conduit.

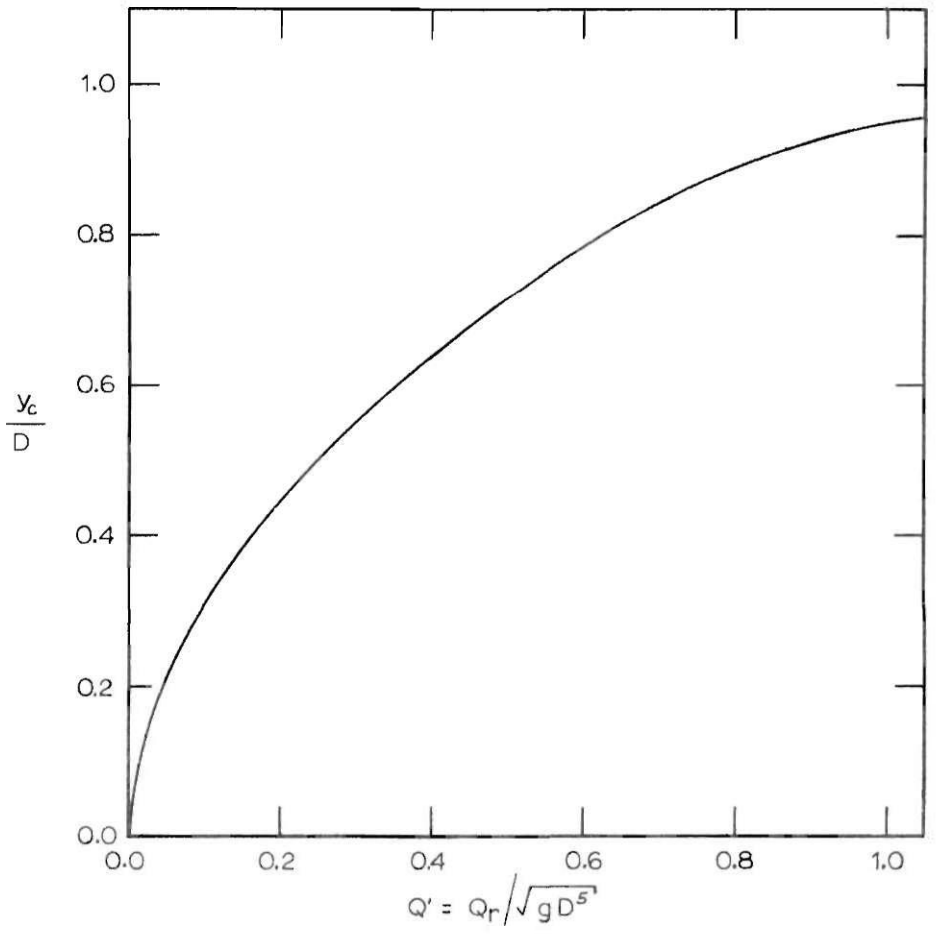

Figure 5. Critical Depth in a Circular Conduit.

CHAPTER III

INSTRUMENTATION AND EQUIPMENT

The equipment used in the research consisted of a channel of circular cross section, a reservoir tank, a wave generator, and a pressure transducer with amplification and recording equipment. All equipment used in the research was available or constructed in the Hydraulics Laboratory of the School of Civil Engineering of the Georgia Institute of Technology.

A 27.810-foot long channel was constructed of cast plexiglass pipe sections connected by flange and bolts. The channel was supported by a steel truss beam on which steel angles were welded and connected to the pipe flanges by bolts. The diameter of the pipe was found to vary along the channel from a maximum of 20.209 centimeters to a minimum of 20.080 centimeters. The average channel diameter was taken as 20.130 centimeters.

One end of the channel was closed by a piston which served as a wave generator. The opposite end of the channel was connected into an open tank constructed of plywood with a steel frame. The open tank was 4.12 feet by 4.40 feet in horizontal cross section. The open tank served three purposes: 1) as end support for the steel truss and channel, 2) as a reservoir, and 3) as an outlet and dissipator for the experimental surges. A one-inch pipe with valve was installed in the bottom of the reservoir tank to serve as outlet and inlet for water level control in the channel.

The closed end of the channel was supported by an adjustable screw jack. Immediately adjacent to the screw jack, the steel truss was bolted to the laboratory floor to pin the truss beam firmly against the screw jack. The screw-jack, bolted-connection system permitted leveling the channel slope. The closed end support is shown in Figure 6 with the wave generator.

In order to counter appreciable center deflections in the beam a one-quarter-inch rod with an adjustable turnbuckle was extended from the ceiling and connected near the center of the beam. The channel was leveled prior to each run after the water level for the next run had been adjusted.

Experimental surges were generated by a plane piston. The plane piston was pushed by a second piston which was two inches in diameter and which was pushed by oil. A positive-displacement oil pump with a constant-speed motor powered the smaller piston. The wave generator and hydraulic driving system are shown in Figure 6. The plane piston was constructed of plexiglass with a soft rubber tube around the perimeter which acted as a gasket. The inside of the circular channel was coated with a lubricant for the length of the maximum stroke. The maximum stroke of the wave generator piston was 4.345 feet.

Wave characteristics were measured from a recording of the pressure difference between two points along the channel as a function of time. Two piezometer openings were constructed in the bottom of the circular at distances of 10.070 feet and 24.185 feet from the closed end of the channel. As an experimental surge passed the first piezometer station the pressure differential between the two piezometer stations would first increase from zero, fluctuate with wave passage, and then stabilize at a

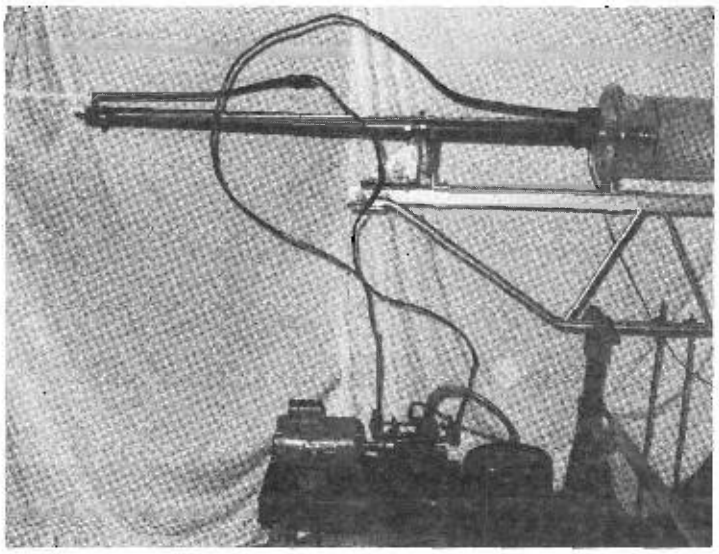

Figure 6. Photograph of Wave Generator.

constant value after the undular waves passed the first piezometer. With a constant pressure differential between the two piezometer stations the process was observed to repeat itself as the surge passed over the second piezometer except the pressure difference decreased toward zero.

To obtain a continuous record of the pressure changes between the two piezometer stations a pressure transducer was employed. Copper tubing served as lines connecting the two piezometer openings with the transducer. A Pace Model KP15 Pressure Transducer was used with a Sanborn Transducer Amplifier Indicator, Model 311A. The Pace Model KP15 is a diaphragm-type transducer by which the deflection of a diaphragm results in a change in inductance ratio between two pickoff coils and the effect is utilized in a bridge circuit to produce an output of voltage proportional to pressure. The amplifier indicator supplies the bridge circuit and must be balanced to compensate for the resistive and capacitive imbalance of the transducer. Graphical recordings of the pressure change with time were performed by a Sanborn Twin-Viso Recorder equipped with a D.C. Amplifier.

Figure 7 is a sample of the recorder output. The output of the recorder was made by the linear movement of special coordinate paper under a transverse deflecting pen which traced on the coordinate paper the load fluctuations of the transducer. A load on the transducer caused the recorder pen to deflect a proportionate distance from a zero position of no load. The zero position of the pen and the range of pen deflection (recorder sensitivity) for expected pressure loads could be controlled. The speed of the recorder paper was constant.

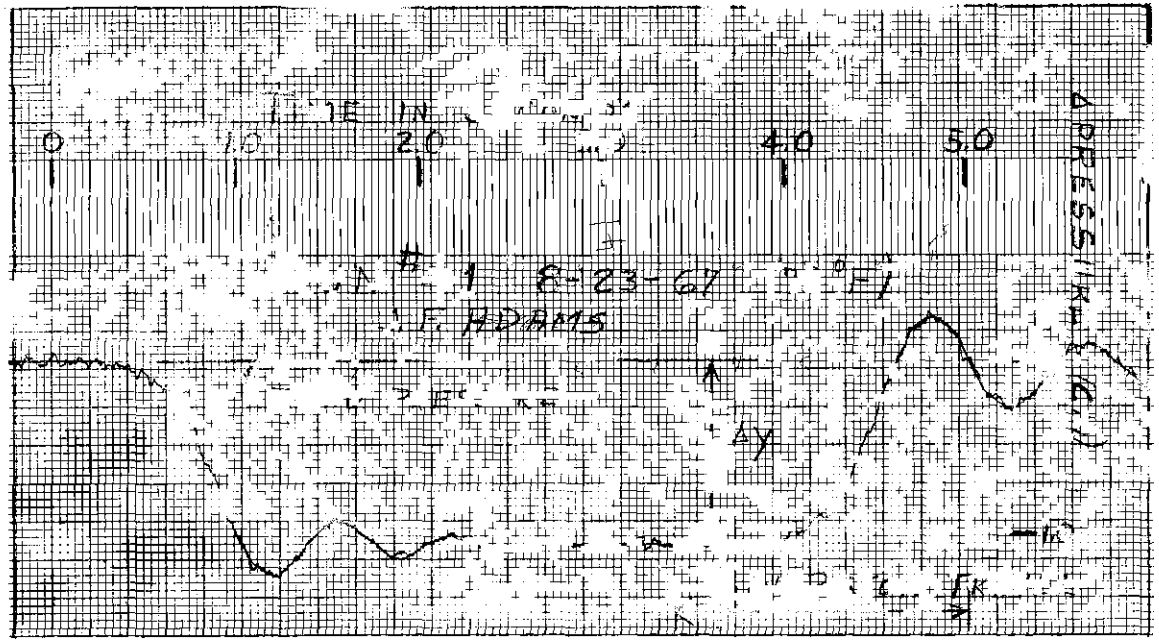

Figure 7. Sample of Recorder Output.

Shown along the bottom of Figure 7 is the track of the timer pen. The recorder timer activated the timer pen at one-second intervals. The recorder paper speed could be determined by measuring the distance on the paper between the one-second marks. The timer pen could also be activated by a micro-switch which sensed the movement of the piston rod of the wave generator in order to obtain an independent determination of the piston speed. The marks along the timer track in Figure 7 were activated by the wave-generator micro-switch.

Figure 8 is a schematic diagram of the laboratory apparatus. Two open manometers of depth capacity greater than the experimental channel diameter were constructed and installed on the side of the reservoir tank. Manometer A was connected to the reservoir tank and served as the depth indicator for the still water level in the channel. Manometer B was connected into a three-way valve and served as means of creating a pressure unbalance in order to calibrate the pressure transducer. Fourteen-millimeter-diameter glass tubes were used for both open manometers in order to minimize meniscus effects. A cathetometer was used to determine the manometer level in relation to the bottom of the channel and to read the water levels in the manometers. The cathetometer enabled water-level readings to be made to the five-thousandths of a centimeter.

A valve-position schedule is shown in Figure 8 along with the schematic diagram of the laboratory apparatus. Three steps, or operations, were necessary to complete a run.

With the three-way valve indicator in Position I, Line 3 was closed and the first piezometer station was linked directly to the

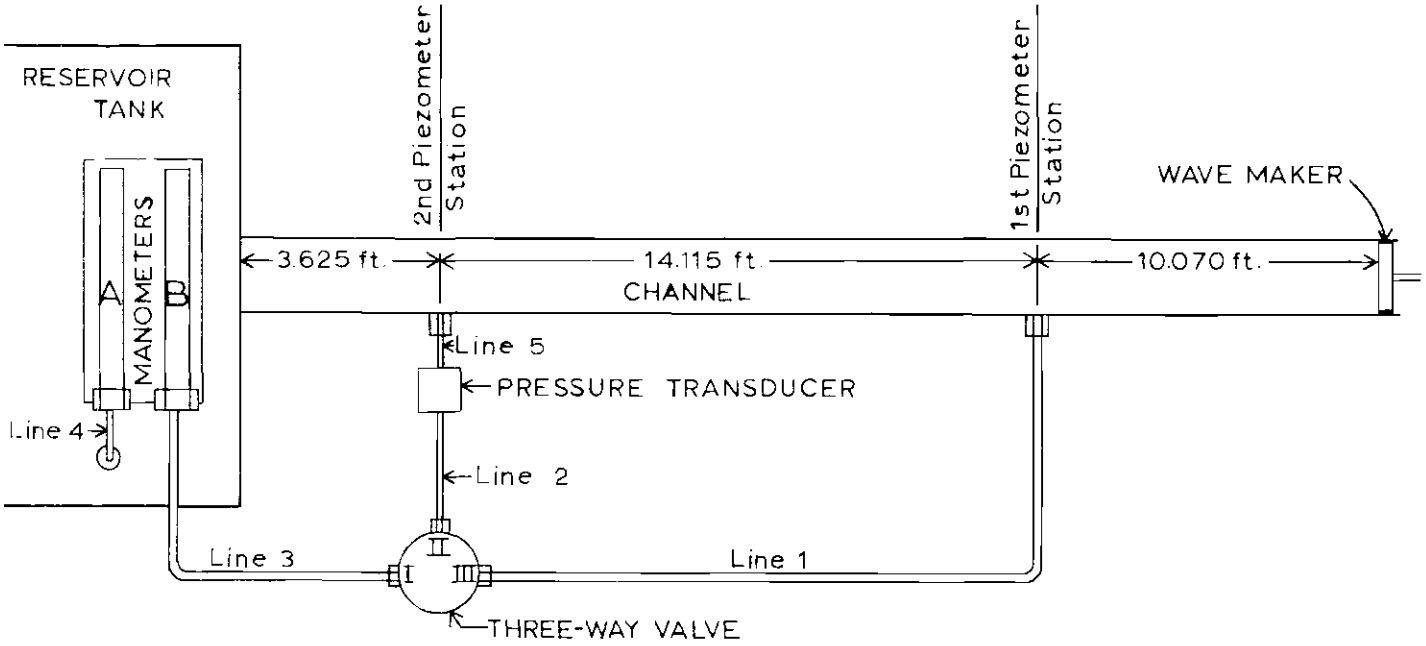

VALVE SCHEDULE			
OPERATION	VALVE POSITION	LINES OPEN	LINES CLOSED
RUN	I	1, 2, 4, 5	3
BALANCE	II	1, 3, 4, 5	2
CALIBRATE	III	2, 3, 4, 5	1

Figure 8. Diagram of Laboratory Apparatus.

pressure transducer through Lines 1 and 2. With this combination the apparatus was set for "run" since the pressure differential across the pressure transducer was the pressure difference between the two piezometer stations. Line 5 connecting the second piezometer station and the pressure transducer remained open during all steps of the experiments.

With the valve indicator in Position II, Manometer B was connected directly to the open channel through Lines 1 and 3. This combination enabled the water levels in the two manometers to balance so that a zero pressure differential could be established across the pressure transducer before calibration of the transducer.

With Position III of the valve indicator, Line 1 was closed and Manometer B was connected directly to the pressure transducer. With Manometer B connected to the pressure transducer, the water level in Manometer B could be changed by adding or deleting small amounts of water through the top of the manometer column. The pressure transducer was calibrated by recording the difference in water levels in the two manometers and the deflection of the recorder pen.

To enable the determination of the velocity of the wave generating piston the one-fourth-inch diameter rod connected to the back side of the plane piston was passed through a stationary micro-switch. The micro-switch was connected to the Sanborn Twin-Viso Recorder so that the recorder timer pen would be activated when the micro-switch was triggered. With movement of the wave generator, the micro-switch was triggered by notches cut in the rod on one-half-foot intervals. From measurements of the recorder paper speed, the distance between each

notch, and the interval between pips on the recorder paper, the piston velocity could be determined. The pips along the bottom of Figure 7 are recordings of 6-inch movements of the piston rod. Maximum speed variation for the piston to travel any one-half foot distance from the average piston speed of any run was of the order of three percent.

Additional equipment used during the experiments consisted of a surveyor's level and a wave dissipator. A surveyor's level was used for leveling of the channel. Accuracy in leveling the channel was estimated at ±0.005 feet but small variations at joints were evident. A wave dissipator was constructed by placing a mat of fibrous material in the reservoir tank against the open end of the circular channel. The wave dissipator was installed to dissipate the wave energy quickly thereby reducing the time between runs.

CHAPTER IV

PROCEDURE

The purpose of the research was to study experimentally surges in an open channel of circular cross section. The investigation was accomplished by conducting laboratory experiments and analyzing the measured and observed results. The equipment used in the experiments is described in Chapter III. All experiments were performed in the Hydraulics Laboratory of the School of Civil Engineering at the Georgia Institute of Technology.

Experiments for the research were conducted in series of usually three to four runs, corresponding to small variation in water depth. During a series of experiments the water level was progressively decreased with each succeeding run by draining water through the outlet pipe in the reservoir tank. By conducting experiments in a series of small-depth variation, the load on the channel due to the weight of the water changed only slightly, thus minimizing time-consuming major adjustments necessary to maintain the horizontal slope of the channel. The procedure of lowering the water level to the desired depth for the following run also proved advantageous in that the channel fluid was disturbed only slightly during drawdown thus shortening the time required between runs for the water to become still. The slope of the channel was checked during each series and was maintained horizontal throughout the experiments.

Before each series of runs the transducer amplifier was balanced and the sensitivity controls of the recorder adjusted to insure the best

graphical recordings of the pressure differential changes between the two piezometer stations located along the channel. During a series of runs the balance of the transducer circuit was checked and rebalanced if necessary.

The execution of a typical run included the following basic steps:

1) calibration of the pressure transducer,

2) determination of the water depth in the open channel,

3) run of the experimental surge, and

4) recalibration of the pressure transducer.

A schematic diagram of the experimental apparatus is shown in Figure 8. The operation of the three-way valve below the pressure transducer is shown on the sketch and is explained in detail in Chapter III.

The calibration of the pressure transducer consisted of establishing a known pressure differential across the transducer and recording the corresponding pen deflection of the recorder. Calibration was performed in the following manner. Once the desired water depth for a respective run was established in the channel, the three-way valve indicator shown in Figure 8 was placed in Position II and the water in the system allowed to calm. With the valve indicator in Position II Manometer B was open directly to the channel. The function of this operation was to balance the two manometers to insure a zero pressure differential across the pressure transducer.

After the water in the system had become calm, the valve indicator was placed in Position III which linked Manometer B directly to the pressure transducer via lines 2 and 3. With the valve indicator in Position III the piezometric head on one side of the transducer was

represented by the water level in the pipe (test section). The piezometric head on the other side of the transducer was represented by the water level in Manometer B. The water level in Manometer B could be changed by addition or subtraction of water and the resulting pressure difference across the transducer determined by noting the difference in the water levels of the two open manometers.

It was noted during trial runs that when the recorder pen was deflected near the paper edge the pen deflection was not proportional to the transducer load. To insure accurate and efficient graphical recordings of the anticipated pressures of a respective surge, the recorder pen was first positioned on the recorder paper when the pressure differential across the transducer was zero. With a zero-pressure differential the recorder was run for a short time, the water levels in the manometers read with a cathetometer, and the respective readings recorded directly on the strip chart. Water was added to or withdrawn from Manometer B. With each pressure differential the recorder was run a short time and the cathetometer reading of the water level in Manometer B recorded. Five to six readings within the range of anticipated pressures were recorded during each calibration for a run.

After calibration of the transducer the two open-column manometers were balanced by placing the three-way valve indicator in Position II. After a short period during which the water in the system was allowed to calm, the valve indicator was placed in Position I which closed Line 3 and opened the first piezometer station directly to the pressure transducer. The channel water level was determined by reading the water level in Manometer A. Each reading made with the cathetometer

was checked after recording the reading. The level of the axis of the cathetometer telescope was checked for each reading.

The electric switch activating the wave generation system was installed adjacent to the recorder and cathetometer to enable one-man operation of the equipment. Immediately before each run, with the valve indicator in Position I and the channel water depth determined, the timer switch of the recorder was activated and the recorder was run for eight to twelve seconds in order to obtain data for paper-speed evaluation. During all the experiments, the maximum deviation from the average paper speed of a respective run from any one second increment of the respective run was of the order of three percent.

Immediately following the time interval for the determination of the recorder paper speed, the timer switch was shut off and the wave generator switch activated thus initiating the respective experimental wave. Each experimental surge could be visually observed for the length of the channel since the channel walls were transparent. Once the surge reached the reservoir end of the channel the wave generator and recorder were de-activated.

After an experimental run the wave generator plane was returned to its original position. Then the water level was lowered to the desired depth of the succeeding run. After the water in the channel had become still, the pressure transducer was recalibrated as previously described. The pressure transducer was calibrated between consecutive runs of a series. Said would serve as the second calibration for the completed run and the first for the next run. Repetition of the pressure-transducer calibration before and after each run was deemed to be prudent

inasmuch as the pressure difference on the channel bottom before and after a surge were very small requiring much amplification of the signal.

The relationship between the recorder pen deflection and the load on the pressure transducer was determined by plotting on arithmetical graph paper the pen deflections recorded during calibration as a function of the corresponding hydrostatic load imposed and drawing a straight line through the plotted points.

Figure 7 is a sample recording from a run. The divisions of the graphical recording paper are one millimeter in length. The pips along the bottom record denote successive 6-inch movements of the piston rod. The jagged line beginning at the left of the figure and continuing across is the graphical record of the differential pressure between the two piezometer stations located along the channel. Entering the left side of Figure 5 the curve maintains a constant mean vertical position indicating the zero pressure differential existing before the wave reached the first piezometer station. With passage of the surge over the first piezometer the depth of water increases. This depth increase is sensed and recorded as a downward plunge, or deflection, of the curve. The wave undulations and the establishment of the final flow depth can be seen. Upon passage over the second piezometer the pressure differential is decreased toward zero as the water level above the two piezometers again are equal.

The data collected from the graphical records were the wave celerity, the final flow depth, and the wave profiles. The wave celerity was calculated from measurements of the horizontal distance on the recording paper between the first peaks recorded at the two piezometers, of the distance between piezometers, and of the speed of movement of the

strip-chart recorder paper. The amplitude of the undular surges and the final water depth were determined by measuring the vertical distance on the recording paper between the desired point and the zero pressure line and by using the pressure-transducer calibration to convert chart deflection to water-depth change. The depth of the initial still water was determined by use of the cathetometer.

CHAPTER V

RESULTS AND DISCUSSION OF RESULTS

Results

The purpose of the research was to investigate small undular surges in an open channel of circular cross section. Experimental surges were generated by means of a constant-velocity plane piston moving into still water. The surges could be visually observed for the length of the channel. Five characteristics of the experimental surges were independently determined as follows: 1) initial water depth, 2) wave celerity, 3) plane piston velocity, 4) final flow depth, and 5) wave profile including the amplitudes of the wave undulations.

All measurements were obtained in a vertical plane along the channel centerline with the result that all data and profiles presented are representative of this vertical plane. For surges of extremely small initial depth, the crest elevations of the wave undulations were visually observed to increase in the transverse direction from a minimum elevation at the channel centerline to a maximum elevation at the section edges. This phenomenon was also believed to be observed of surges of depth approaching the channel diameter. However, since these surges traveled with extremely high celerities, only a brief time period was available for observation.

Positive surges were generated in the circular conduit with initial still-water depth being the variable from run to run. All surges investigated retained a complete free surface for the length of the

channel. All surges generated were smooth undular. Experimental results are listed in Table 1. The five columns in Table 1 are run number, still-water depth before the surge, uniform steady flow depth behind the surge, surge celerity, and piston velocity reading from left to right. Surge profiles of Runs 23, 7, 21, and 20 are reproduced in Figures 9, 10, 11, and 12, respectively. Each figure exhibits two profiles of a run. The uppermost profile is the wave configuration as recorded at a point 10.070 feet from the closed end of the channel. The lower profile is the wave configuration as recorded with wave passage over a point 24.185 feet from the closed end of the channel. The profiles in Figures 9, 10, 11, and 12 are tracings of the laboratory recordings of the pressure differential changes between the two defined points. The vertical axis is linearly proportional to the height of the physical wave above the initial still water surface. The horizontal axis is in seconds.

Analysis of Results

Control-Volume Analysis

Control-volume or one-dimensional analysis is a simple but powerful method of analyzing flow phenomenon for which the upstream and downstream sections of the control volume can be located in uniform flow zones. Control-volume analysis of the surge was presented in Chapter II, THEORY in which the equation of continuity and one equation of linear momentum (along the conduit axis) were derived. By neglecting the boundary-shear force on the periphery of the control volume, definitive equations about pressure-plus-momentum, Equations 13 and 16, and for surge celerity, Equation 7, were derived.

Table 1. Experimental Results

Run No.	y_1/D	y_2/D	c (cm/sec)	V_p (cm/sec)
25	0.108	0.126	41.9	9.02
24	0.121	0.140	44.3	9.02
23	0.140	0.162	47.7	9.02
8	0.182	0.208	54.7	9.05
7	0.222	0.248	60.6	9.02
21	0.251	0.279	64.1	8.97
20	0.352	0.386	76.9	9.02
19	0.445	0.483	86.8	8.96
18	0.498	0.538	92.6	8.93
17	0.596	0.640	104	8.93
42	0.626	0.675	109	9.39
41	0.701	0.755	119	9.39
40	0.750	0.806	126	9.36
38	0.816	0.877	139	9.27
37	0.846	0.910	148	9.30
36	0.878	0.947	160	9.24

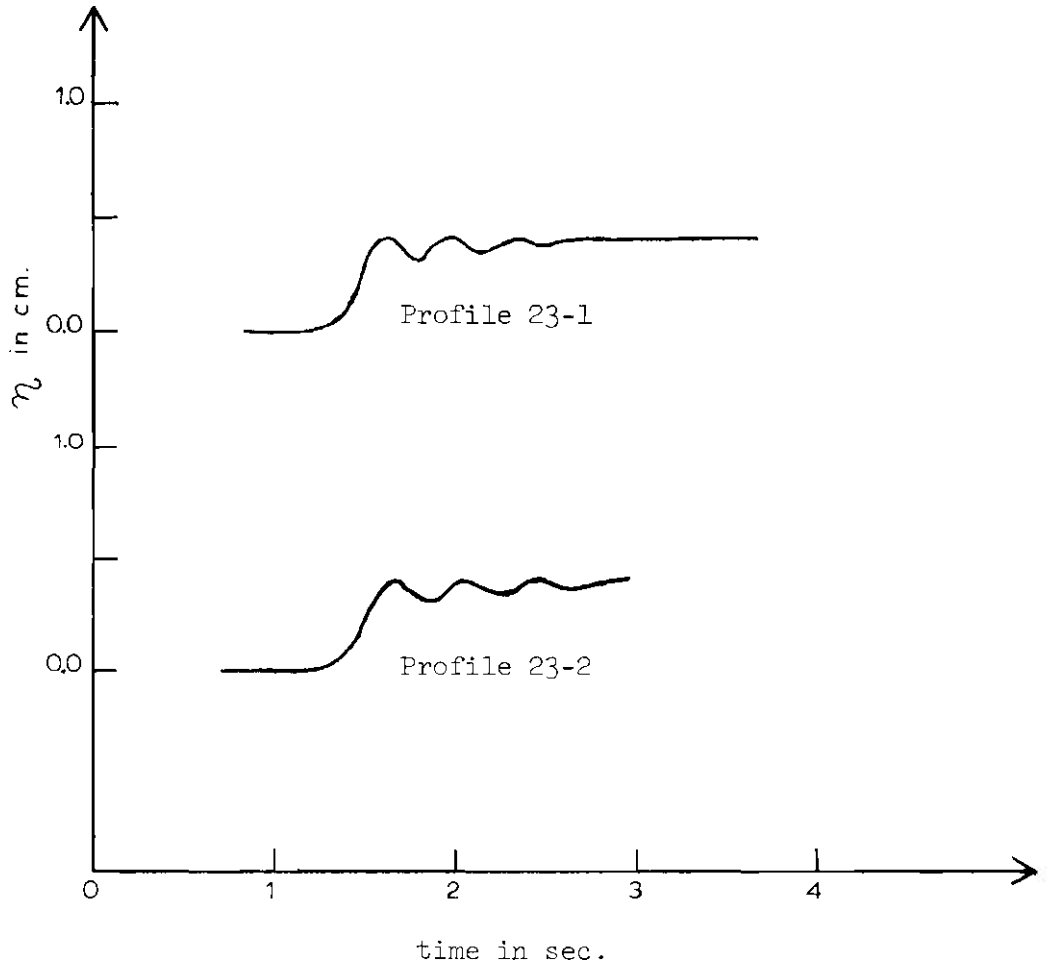

Figure 9. Profiles of Run No. 23.

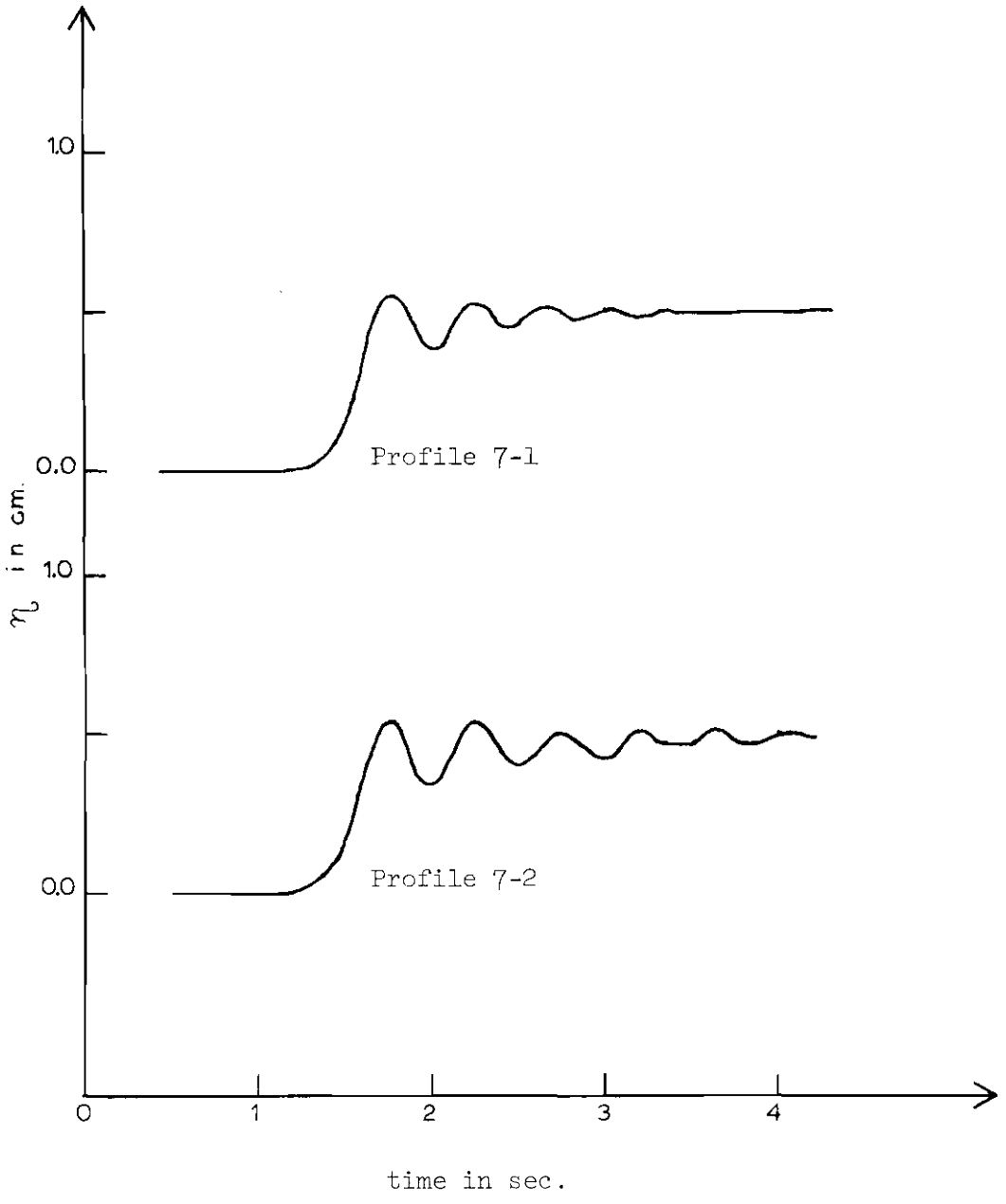

Figure 10. Profiles of Run No. 7.

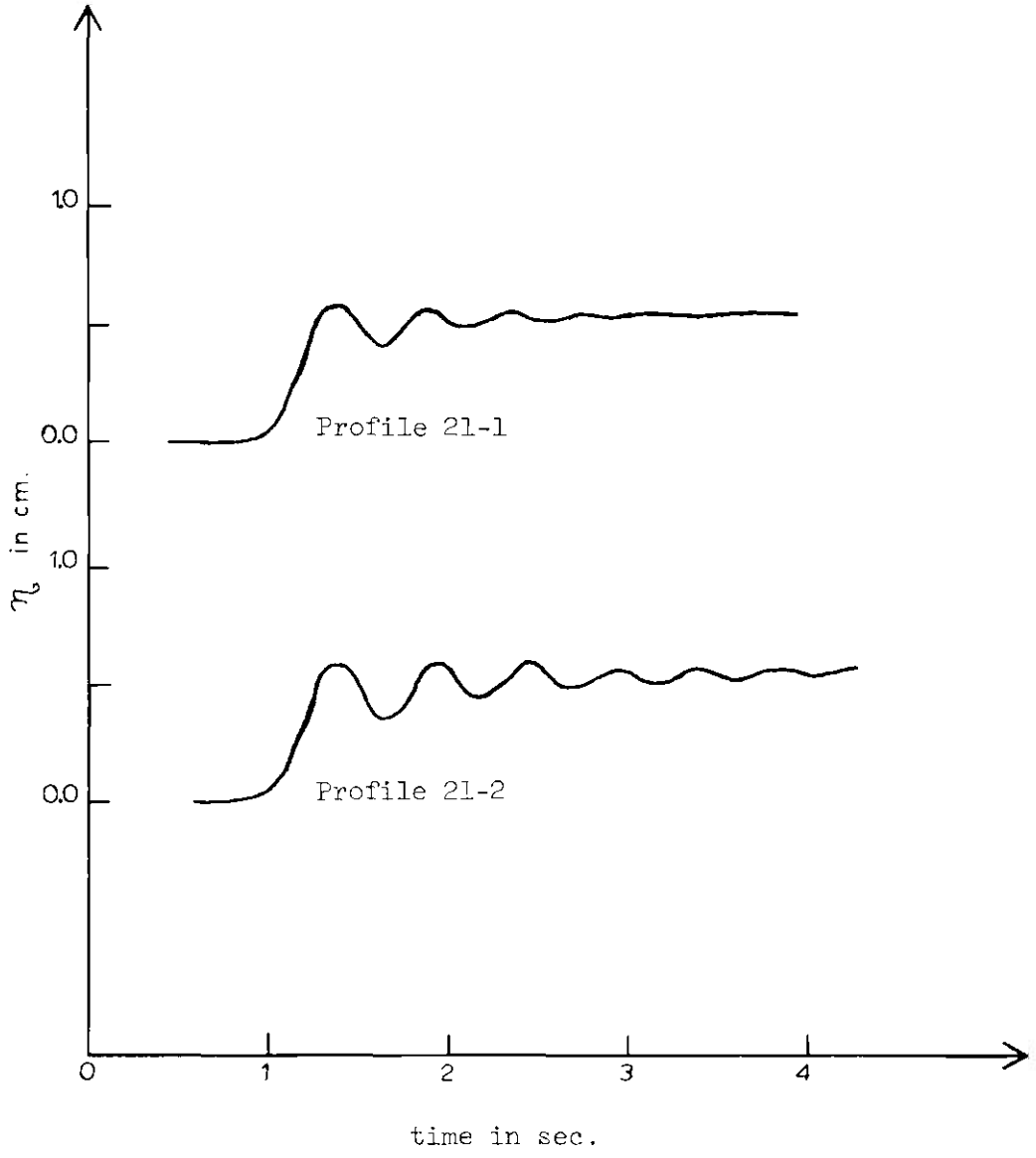

Figure 11. Profiles of Run No. 21.

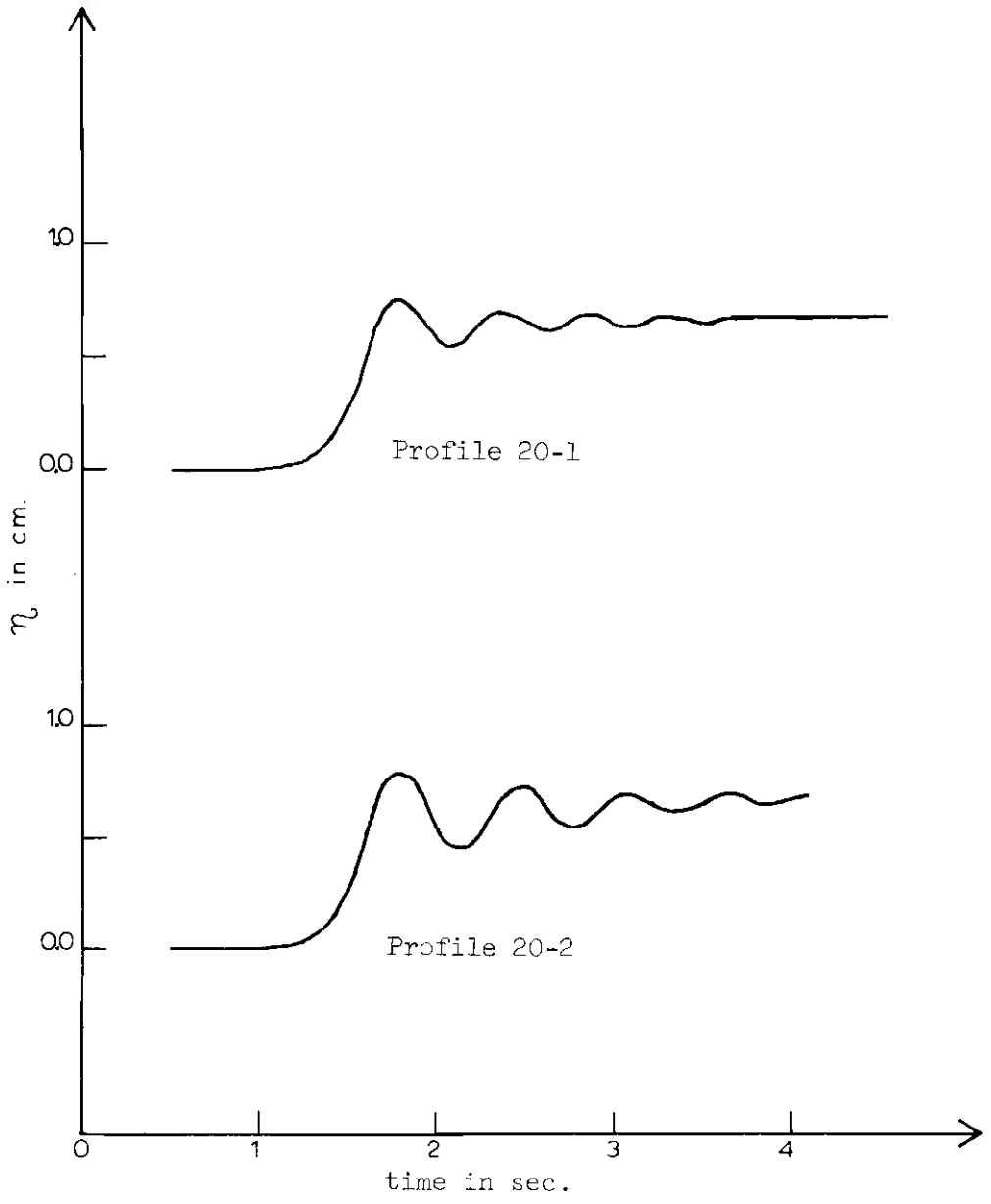

Figure 12. Profiles of Run No. 20.

By neglecting the boundary-shear force, F_f, in Equation 5, theoretical analysis is indicative that the pressure-plus-momentum before and behind the surge are equal, Equation 13. Of course this result is valid only if the coordinate system is attached to the surge front. A curve of pressure-plus-momentum was calculated using Equation 16 for each of the 16 runs listed in Table 1. The value of Q_r was computed from Equation 4a using the values of c and A_1 determined from experimental measurements. These curves are shown in Figures 13(a) and 13(b). After the curves were calculated and plotted, the depths, y_1/D and y_2/D, as listed in Table 1 were plotted on the appropriate curve. These experimental points are designated by circles in Figures 13(a) and 13(b). If the boundary-shear force is zero as assumed in the derivation of Equation 13, the two points of each run would lie on the same vertical line in Figure 13. Using this criterion, the boundary-shear force does appear to be truly negligible for values of $Q' > 0.070$ and $y_1/D > 0.3$. On the other hand, the pressure-plus-momentum is observably greater behind the surge in the runs in which $y_1/D < 0.3$. The pressure-plus-momentum behind the surge is expected to be somewhat greater than in front of the surge by virtue of the direction of the boundary-shear force shown in Figure 2. The magnitude and direction of F_f is exactly the same in the fixed coordinate system, Figure 1, as in the moving coordinate system, Figure 2. In any event, no general rule as to whether the pressure-plus-momentum increases or decreases through a surge is possible inasmuch as F_f can be in the opposite direction as, for example, in the stationary surge or hydraulic jump.

Equation 7 was derived for surge celerity also by neglecting the

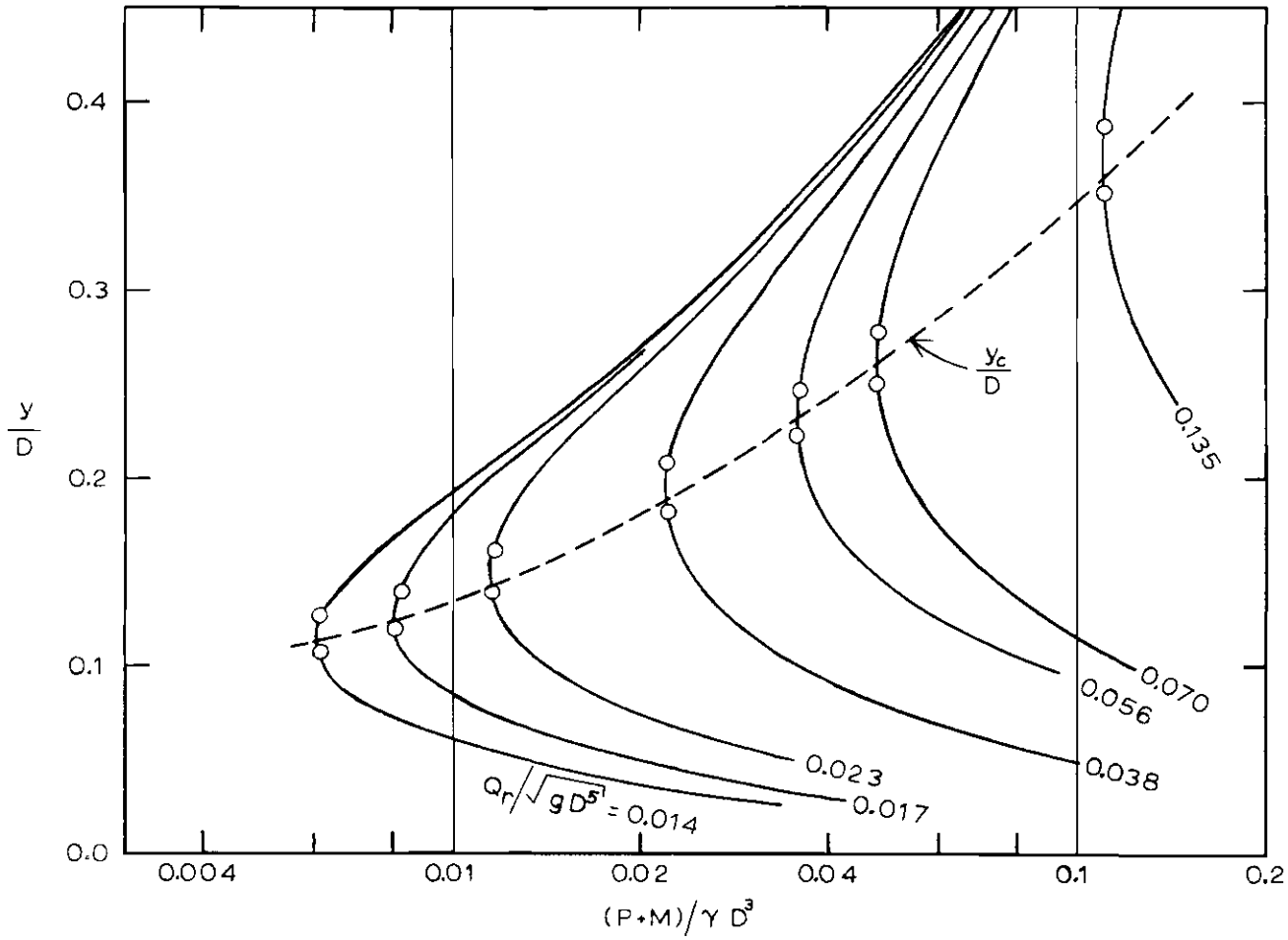

Figure 13(a). Pressure-plus-Momentum (Experimental Results).

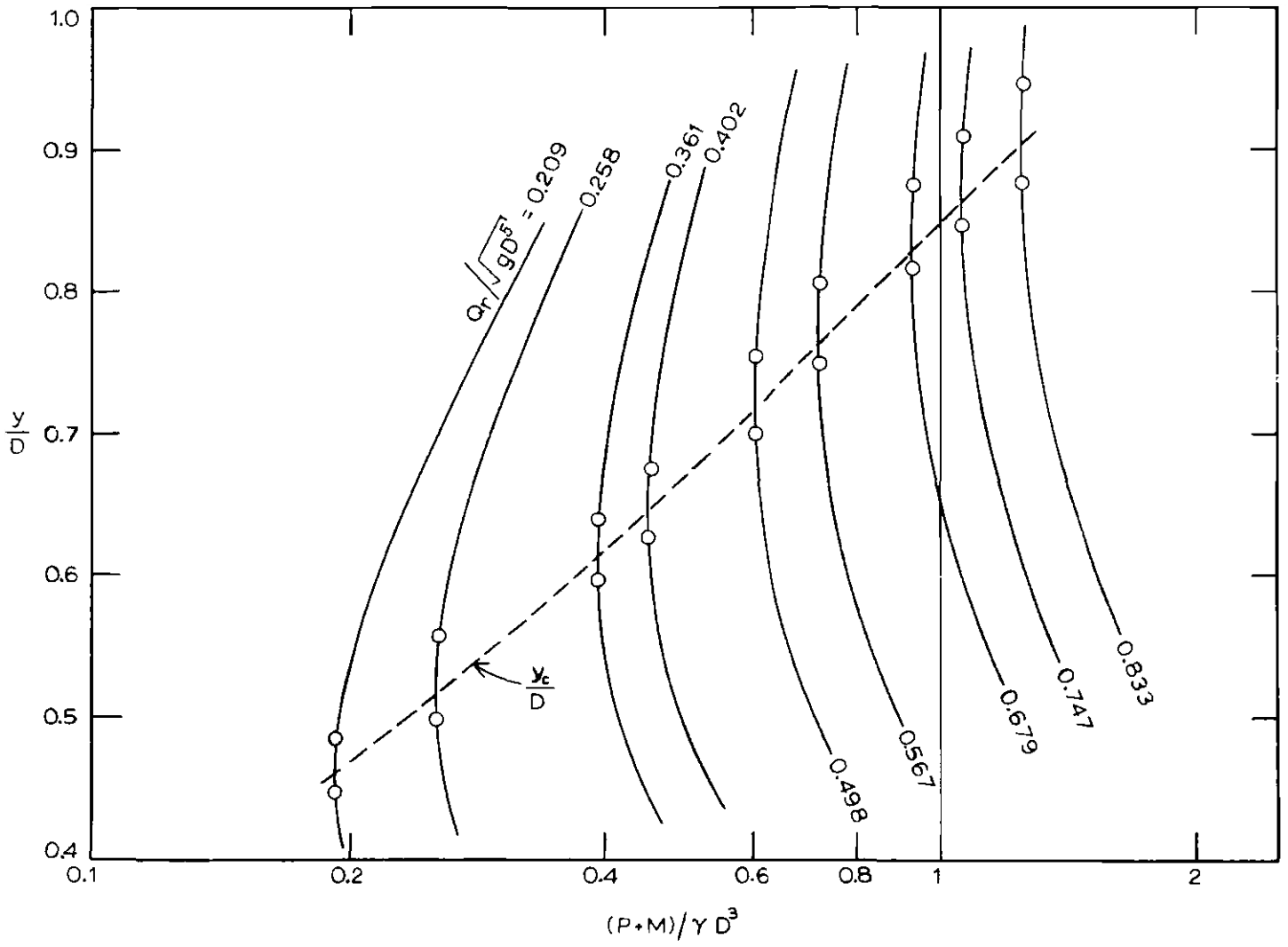

Figure 13(b). Pressure-plus-Momentum (experimental Results).

boundary-shear force. Curves for surge celerity at constant values of $\Delta y/D$ or $(y_2 - y_1)/D$ were computed using Equation 7 and are plotted in Figure 14. Surge celerity obtained from experimental measurements are plotted as circular points on Figure 14. Theoretical values neglecting F_f for the values of y_1/D and $\Delta y/D$ of each run are also shown in Figure 14. In every case the surge celerity determined from experimental measurements is slightly less than the theoretical value. In the mid-depth range, $0.25 < y_1/D < 0.75$, the experimentally determined values are less than 3 per cent lower than the theoretical values. That the experimentally determined values of celerity are somewhat lower is to be expected. If the boundary-shear force is not neglected in Equation 5, the solution for celerity corresponding to Equation 7 is as follows

$$c = \sqrt{g\bar{y}_1}\,\frac{\left(\frac{A_2\bar{y}_2}{A_1\bar{y}_1} - 1 - \frac{F_f}{\gamma A_1\bar{y}_1}\right)^{\frac{1}{2}}}{\left(1 - \frac{A_1}{A_2}\right)^{\frac{1}{2}}} \qquad (18)$$

The effect of including the boundary-shear force, F_f, in theory is shown by Equation 18 to result in a lower theoretical value of surge celerity. Refinement of the theoretical solution to include a rational expression for F_f is not feasible inasmuch as the flow under the surge front (within the control volume) is very non uniform with the overriding flow, $V_w(A_2-A_i)$, in Figure 1 entraining the underlying water in a short distance so that the entire stream has a common velocity V_2 behind the surge.

Surge Profiles

All information about the water-surface profile in the surge must

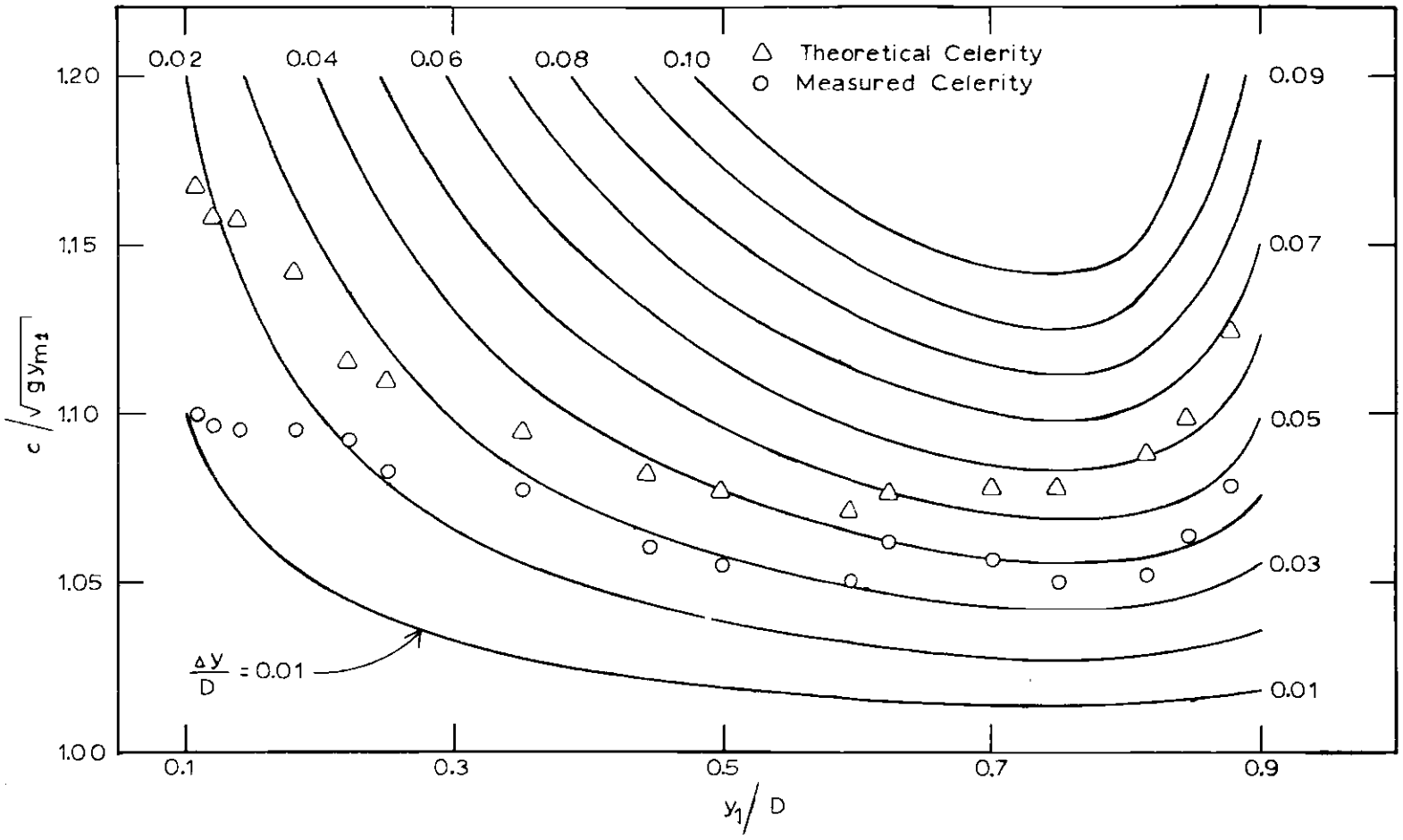

Figure 14. Surge Celerity.

be obtained experimentally because the control-volume analysis includes too many unknown variables to be useful in the non uniform flow under the smooth undulating surge. Study of the profiles of Figures 9, 10, 11, and 12 is indicative that the water-surface profile changes between the two cross sections where the piezometers are located. In general the elevation of the first crest above still-water water level is higher at piezometer 2 than at piezometer 1 as shown in Figure 15. Also the elevation of the first trough is lower at piezometer 2 than at piezometer 1 as shown in Figure 16. In addition the wave length of the undulations and the number of undulations were found to be greater at piezometer 2 than at piezometer 1. These changing conditions are probably the result of the continually increasing length between section 2 behind the surge and the piston face. The increasing length of water mass moving in the direction of the piston necessarily results in an increase in the boundary-shear force between section 2 and the piston face.

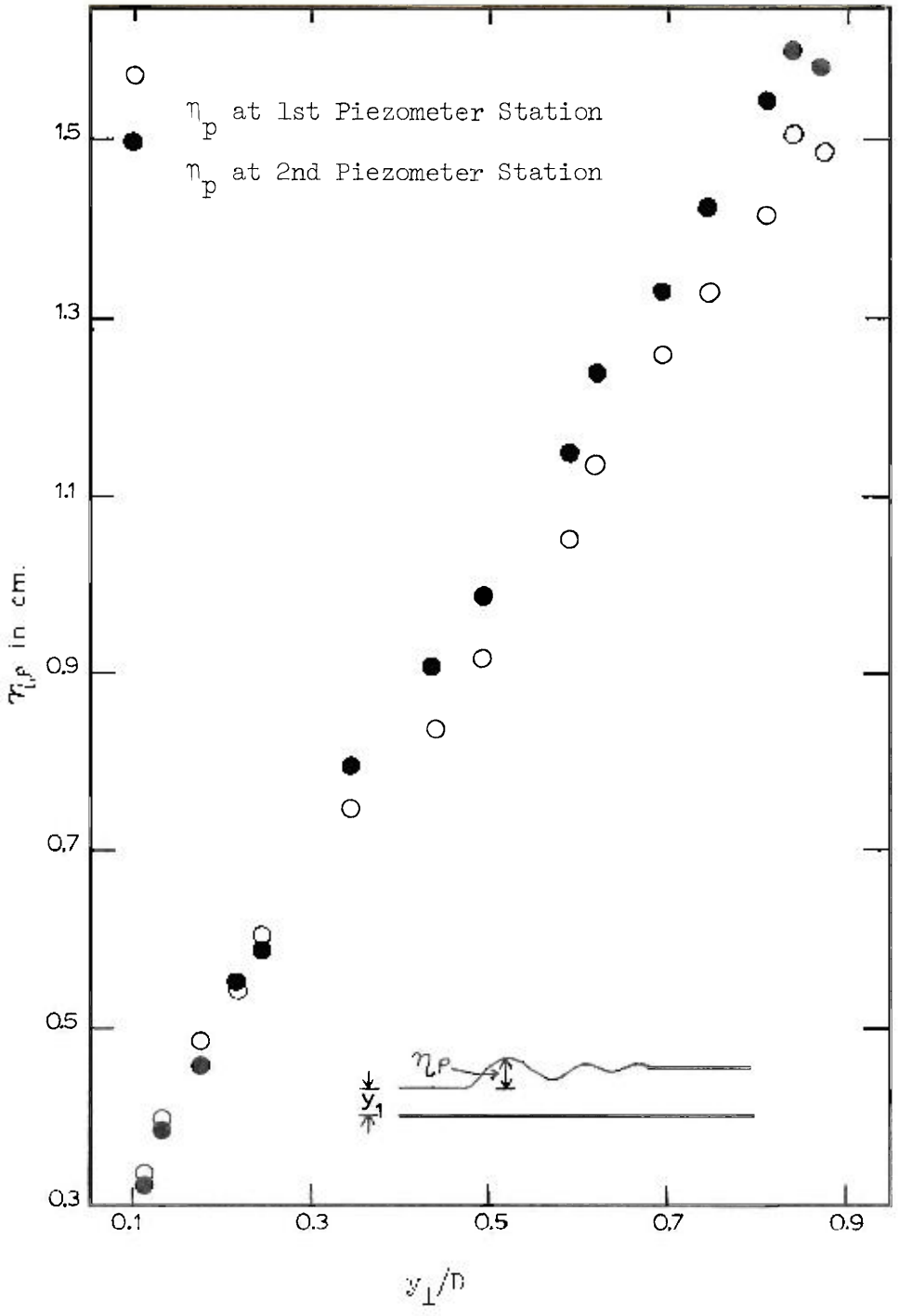

Figure 15. First-Undulation Crest Height.

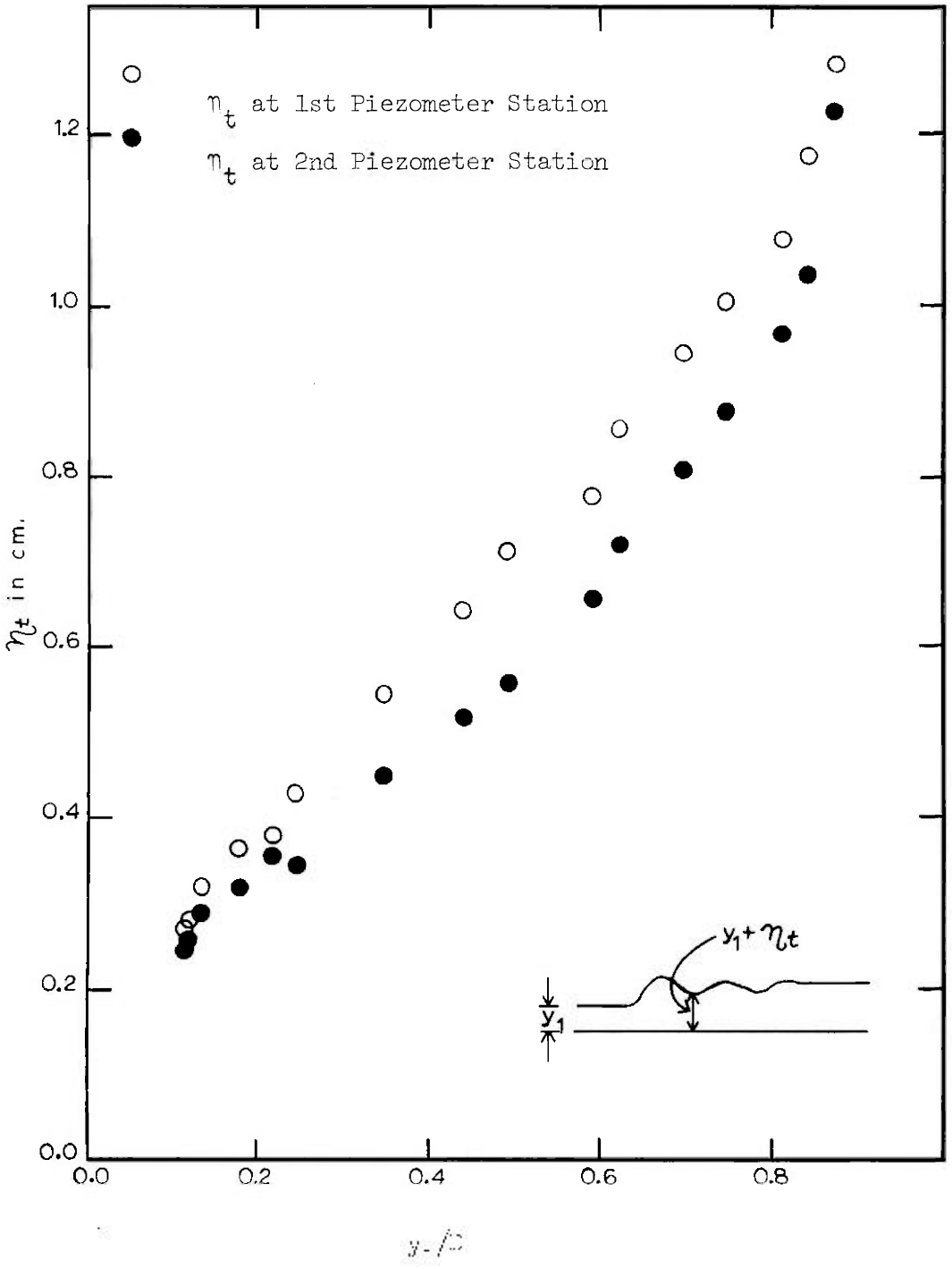

Figure 16. First-Undulation Trough Height.

CHAPTER VI

CONCLUSION

This series of experiments with a positive surge in a circular-segment open channel has demonstrated the validity of one-dimensional analysis in a nonrectangular channel in which cross-channel transfers of linear momentum exist through the surge. As a corollary the use of the hydraulic mean depth, $y_m = A/T$, was found to be a valid depth to be used in the computation of wave celerity, Froude numbers, and so forth in spite of the seemingly preposterous values of y_m as the water surface approaches the top of the circular conduit.

LITERATURE CITED

1. G. H. Keulegan, "Wave Motion." In Engineering Hydraulics (Hunter Rouse, ed.) New York: John Wiley & Sons, Inc., 1950, pp. 749-750.

2. A. M. Binnie and J. C. Orkney, "Experiments on the Flow of Water from a Reservoir Through an Open Horizontal Channel: II, The Formation of Hydraulic Jumps," Proceedings, Royal Society of London, Ser. A, Vol. 230, No. 1181, 1955, pp. 237-246.

3. O. C. Zienkiewicz and J. A. Sandover, "The Undular Surge Wave," Proceedings of the Seventh Congress, International Association for Hydraulic Research, Lisbon 1957, Vol. 2, 1957, pp. D25-1 to D25-6.

4. E. W. Lane and C. E. Kindsvater, "Hydraulic Jump in Enclosed Conduits," Engineering News-Record, Vol. 121, Dec. 29, 1938, pp. 815-817.

5. J. A. Sandover and C. Taylor, "Cnoidal Waves and Bores," La Houille Blanche, Vol. 17, No. 3, July-August, 1962, pp. 443-455.

6. Robert David Wilroy, "An Investigation of the Critical Depth in an Open Channel with a Non-Rectangular Cross Section," M.S. Thesis, Georgia Institute of Technology, 1954.

7. A. J. Rodrigues-Diaz, "The Hydraulic Jump in a Non-Rectangular Open Channel," M.S. Thesis, Georgia Institute of Technology, 1955.

APPENDIX -- NOTATION

The following symbols are used in this paper:

A = cross-sectional area;

A_p = cross sectional area at face of piston;

c = wave celerity;

D = channel cross-sectional diameter;

F_f = boundary-shear force;

g = acceleration of gravity;

P = hydrostatic pressure force;

$P+M$ = pressure-plus-momentum;

Q_r = relative discharge, cA_1;

Q' = $Qr/\sqrt{gD^5}$;

T = section top width;

V = flow velocity;

V_p = plane piston velocity;

V_w = absolute wave velocity;

y = flow depth;

y_c = critical depth;

$\overline{y}$ = distance from free surface to centroid of cross section;

y_m = mean depth, A/T;

y_{m1} = initial mean depth, A_1/T;

y_1 = initial flow depth;

y_2 = final flow depth;

Δy = $y_2 - y_1$;

α = (alpha) see Figure 3;

γ = (gamma) unit weight of water;

η = (eta) height of wave surface above initial still water;

η_p = (eta) height of first undulation crest above initial still water;

η_t = (eta) height of first undulation trough above initial still water;

ρ = (rho) density of water; and

$\mathbb{F}$ = Froude number.